

## Magnetoplasma excitations in quantum-well wires

L. Wendler and V. G. Grigoryan

*Fachbereich Physik, Martin-Luther-Universität Halle, Friedemann-Bach-Platz 6, D-06108 Halle, Federal Republic of Germany*

(Received 4 January 1994)

The spectrum of the collective excitations of a magnetoplasma, confined in a quasi-one-dimensional quantum-well wire is analyzed. The dispersion relations of the intrasubband and intersubband magnetoplasmons are calculated with excellent agreement to experimental results. The calculations are done in the random-phase approximation with no further simplifying approximation. We find analytical results for the dispersion relations of the intrasubband and intersubband magnetoplasmons.

The spectrum of the collective excitations of a quasi-one-dimensional electron gas (Q1DEG) in the absence<sup>1-5</sup> and in the presence of a quantizing magnetic field<sup>6-13</sup> has been explored theoretically<sup>1-9</sup> and experimentally.<sup>10-13</sup> Some fundamental questions about the many-particle behavior of the Q1DEG remain open up to now. One of these is the question of whether the Q1DEG is better described as a Fermi liquid, or if the model of a Tomonaga-Luttinger liquid is more appropriate. In fact, the strictly 1D Fermi system is a singular, strongly correlated many-body system where any interaction between the electrons leads to essential singularities. But on the other hand, experimental results<sup>10-13</sup> and theoretical investigations<sup>14</sup> show that the Q1DEG is quantitatively well described by the random-phase approximation (RPA), i.e., in the lowest order of the Feynman-Dyson perturbation series of a Q1D Fermi liquid. Also in the case where exchange-correlation effects, ignored in the RPA, become important the Fermi-liquid model treated within the time-dependent Hartree-Fock approximation is appropriate to describe the resulting effects.

In this paper, we present a quantum theory of Q1D magnetoplasmons in quantum-well wires (QWW) within the RPA, without further approximations on the RPA. Hence, our theory is valid for all wave vectors, magnetic-field strengths, and electron densities as long as the RPA is valid. We study the single QWW by a model in which the electrons are confined in a zero-thickness

$x$ - $y$  plane along the  $z$  direction at  $z=0$ . In the  $y$  direction the electron motion is quantum-confined by an effective potential, assumed to be parabolic:  $V_{\text{eff}}(y)=m\Omega^2 y^2/2$ . Choosing the Landau gauge  $\mathbf{A}=(-yB,0,0)$  for the vector potential of the external applied magnetic field  $\mathbf{B}=(0,0,B)$  and ignoring the Zeeman spin splitting, the single-particle Hamiltonian is exactly solvable with the single-particle wave function  $\langle \mathbf{x}|N, k_x \rangle = \Psi_{Nk_x}(\mathbf{x}) = 1/\sqrt{L_x} e^{ik_x x} \Phi_N(y - Y_{k_x}) \varphi(z)$ , where  $\Phi_N(y - Y_{k_x})$  is the shifted harmonic-oscillator wave function. The corresponding energy eigenvalues are  $\mathcal{E}_N(k_x) = \hbar\tilde{\omega}_c(N + \frac{1}{2}) + \hbar^2 k_x^2 / 2\tilde{m}$ ;  $N=0, 1, 2, \dots$ . In these equations the center coordinate is  $Y_{k_x} = \gamma \tilde{l}_0^2 k_x$ , where  $\tilde{l}_0 = (\hbar/m\tilde{\omega}_c)^{1/2}$  is the typical width of the wave function and  $\gamma = \omega_c / \tilde{\omega}_c$ . Further,  $\tilde{\omega}_c = (\omega_c^2 + \Omega^2)^{1/2}$  is the hybrid frequency,  $\omega_c = eB/m$  is the cyclotron frequency, and  $\tilde{m} = m(\tilde{\omega}_c/\Omega)^2$  is the renormalized magnetic-field-dependent mass.

The single-particle Hamiltonian of the electrons of the Q1DEG in the presence of an external perturbation is written as  $H = H_0 + H_1$ , where  $H_0$  is the unperturbed Hamiltonian and  $H_1 = V^{\text{sc}}(\mathbf{x}, t)$  is the self-consistent potential. This perturbation induces an electron number density which is related to the self-consistent potential by the irreducible polarization function  $P^{(1)}(q_x; \mathbf{x}_1, \mathbf{x}'_1 | \omega)$  of the Q1D magnetoplasma

$$P^{(1)}(q_x; \mathbf{x}_1, \mathbf{x}'_1 | \omega) = \sum_{N, N'} \sum_{k_x} P_{NN'}^{(1)}(q_x, k_x | \omega) \Phi_N(y - Y_{k_x + q_x}) \Phi_{N'}^*(y' - Y_{k_x + q_x}) \Phi_N(y' - Y_{k_x}) \Phi_{N'}^*(y - Y_{k_x}) \delta(z) \delta(z'), \quad (1)$$

with  $\mathbf{x}_1 = (0, y, z)$  and where  $P_{NN'}^{(1)}(q_x, k_x | \omega)$  is the RPA matrix polarization function at  $T=0$  K.<sup>3</sup> In the presence of a quantizing magnetic field, applied in  $z$  direction the wave function describing the electron motion in  $y$  direction depends on  $k_x$ . If we proceeded in the standard manner of the linear-response theory to derive the dispersion relation of the Q1D magnetoplasmons we would have to solve an infinite-dimensional secular equation according to  $k_x$ . Hence, to obtain the exact RPA dispersion relation in the subband space we use the following representation of the shifted harmonic-oscillator wave function:<sup>7</sup>  $\Phi_N(y - Y_{k_x}) = \sum_{L=0}^{\infty} C_{LN}(Y_{k_x}) \Phi_L(y)$ , where

$\{\Phi_N(y)\}$  is a closure set of undisplaced wave functions. Li and Das Sarma<sup>6</sup> proposed a different perturbation expansion scheme, the  $\alpha$  expansion. Differing with the representation used here the  $\alpha$ -expansion scheme is restricted to very small electron densities and weak or strong magnetic fields. Unfortunately, this expansion is not valid in the range of the parameters, used in experiments,<sup>10-13</sup> e.g., it breaks down for a typical QWW with  $\hbar\Omega = 2$  meV and  $n_{\text{1DEG}} = 1 \times 10^6$  cm<sup>-2</sup> between  $B = 0.3$  T and  $B = 20$  T.

In the RPA and neglecting retardation effects the induced density is related to the induced potential by

Poisson's equation. Assuming a constant background dielectric constant  $\epsilon_s$  in the region of the Q1DEG, the dispersion relation of the collective excitations of the Q1D magnetoplasma follows in the form

$$\det[\delta_{LL'}\delta_{L'L_2} - \Xi_{L_1L_2LL'}(q_x, \omega)] = 0, \quad (2)$$

where  $\Xi_{L_1L_2LL'}(q_x, \omega) = \Lambda_{L_1L_2LL'}(q_x, \omega)$  if  $L = L'$ , and  $\Xi_{L_1L_2LL'}(q_x, \omega) = \Lambda_{L_1L_2LL'}(q_x, \omega) + \Lambda_{L_1L_2L'L}(q_x, \omega)$  if  $L \neq L'$ . In this equation we have defined

$$\Lambda_{L_1L_2LL'}(q_x, \omega) = \sum_{L_3L_4} V_{L_1L_2L_3L_4}^s(q_x) \mathcal{P}_{L_3LL'L_4}^{(1)}(q_x, \omega), \quad (3)$$

$$V_{L_1L_2L_3L_4}^s(q_x) = \frac{e^2}{2\pi\epsilon_0\epsilon_s} (-1)^{L_1+L_2} e^{a\sqrt{L_1!L_2!L_3!L_4!}}$$

$$\times \sum_{m_2=0}^{L_2} \sum_{m_4=0}^{L_4} \sum_{\nu=0}^{\lambda} (-1)^\nu \frac{a^\lambda C_\nu^\lambda (2\lambda-1)!! K_\nu(a)}{m_2!m_4!(L_2-m_2)!(L_4-m_4)!(L_1-L_2+m_2)!(L_3-L_4+m_4)!(\lambda-\nu)!}, \quad (5)$$

with  $a = (\bar{l}_0 q_x / 2)^2$ ,  $\lambda = m_2 + m_4 + (L_1 - L_2 + L_3 - L_4) / 2$ ,  $C_\nu^\lambda = \frac{1}{2}$  for  $\nu=0$  and  $C_\nu^\lambda = 1 / [(\lambda+1) \dots (\lambda+\nu)]$  for  $\nu \neq 0$ , and  $K_\nu(y)$  is a modified Bessel function.

For numerical work we have chosen a GaAs-Ga<sub>1-x</sub>Al<sub>x</sub>As QWW (GaAs:  $\epsilon_s = 12.87$  and  $m = 0.06624m_0$ ) using a three-subband model, i.e.,  $N, N' = 0, 1, 2$  from which the lowest is assumed to be occupied in equilibrium.

In Fig. 1 the full RPA dispersion relations of the magnetoplasmons of the three-subband model are plotted for a QWW using Eq. (2), in dependence of the wave vector [Fig. 1(a)] and of the magnetic field [Fig. 1(b)]. The (0-0), (1-0), and (2-0) magnetoplasmons are coupled excitations, with one intrasubband branch  $\omega_{mp}^{00}$  and two intersubband

with

$$\begin{aligned} \mathcal{P}_{L_3LL'L_4}^{(1)}(q_x, \omega) &= \sum_{NN'} \sum_{k_x} P_{NN'}^{(1)}(q_x, k_x | \omega) \\ &\times C_{L_3N}(Y_{k_x+q_x}) C_{LN}^*(Y_{k_x+q_x}) \\ &\times C_{L'N'}(Y_{k_x}) C_{L_4N'}^*(Y_{k_x}) \end{aligned} \quad (4)$$

and the matrix elements of the Coulomb interaction potential read

branches,  $\omega_{mp}^{10}$  and  $\omega_{mp}^{20}$ . The shaded areas are the corresponding single-particle intrasubband and intersubband continua in which the modes become Landau damped. The frequency  $\omega_{mp}^{00}$  of the intrasubband magnetoplasmon increases with the increasing wave-vector component  $q_x$  but decreases with the increasing magnetic field. Such a behavior is known from the edge modes of a spatially confined Q2DEG. Hence, the Q1D intrasubband magnetoplasmon behaves like an edge mode. Further, it is seen that the two intersubband branches are depolarization shifted. The dispersion curves of the intersubband magnetoplasmons  $\omega_{mp}^{N0}$  approach, for large magnetic fields, multiples of the cyclotron frequency. In the same limit the single-particle intersubband continua degenerate to

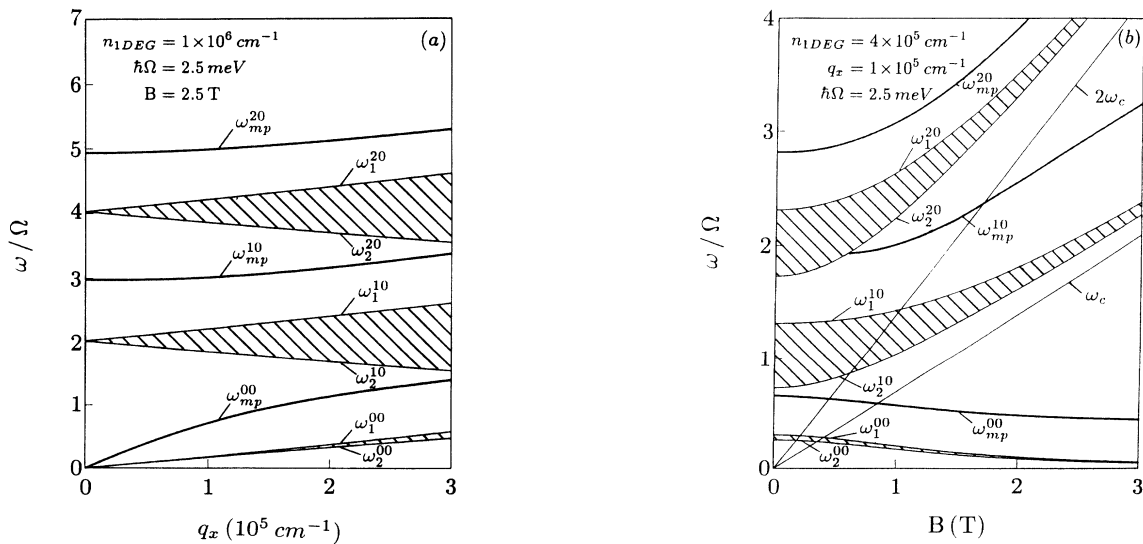


FIG. 1. Dispersion relation of the mixed (0-0)-(1-0)-(2-0) magnetoplasmons calculated in RPA (solid lines) of a GaAs-Ga<sub>1-x</sub>Al<sub>x</sub>As QWW for a three-subband model, where one subband is occupied as a result of dependence on the wave-vector component  $q_x$  (a) and the magnetic field (b). The shaded areas correspond to the single-particle intrasubband and intersubband continua with the boundaries  $\omega_{1,2}^{N0} = |\pm \hbar k_F^{(0)} q_x / \bar{m} + \hbar q_x^2 / (2\bar{m}) + N\bar{\omega}_c|$ .

single lines at  $N\omega_c$ . Following, the Q1D magnetoplasma behaves like a 2D magnetoplasma, where the (1-0) intersubband branch goes over to the principal mode and the higher intersubband branches to Bernstein modes. For very large magnetic fields all modes are free of Landau damping because of the complete quantized situation. It is important to note that there are additional modes in the spectrum of the intersubband magnetoplasmons not plotted in Fig. 1. These modes have smaller depolarization shifts than the plotted modes, i.e., are slightly above the intersubband continua. Further, the additional intersubband magnetoplasmons depend on higher order on the magnetic field:  $\omega_{mp}^{NO} \propto N\omega_c + O(B^4)$ .

In Fig. 2 the RPA dispersion curve of the intrasubband magnetoplasmon  $\omega_{mp}^{00}$  is plotted versus magnetic field. The edge mode behavior of this branch is evident. In addition to the calculated dispersion curve the experimental results of Demel *et al.*<sup>11</sup> are plotted. The quantitative comparison of the theoretical results for the (0-0) intrasubband magnetoplasmon of a three-subband model with experiments on samples where between one and six subbands are occupied, depending on the magnetic field, is possible because the dispersion relation of the (0-0) intrasubband magnetoplasmon only depends on the total electron density.<sup>15</sup> It is seen from Fig. 2 that the developed model well describes the experimental results.

Figure 3 shows dependence of the RPA dispersion relation of the (1-0) intersubband magnetoplasmon  $\omega_{mp}^{10}$  on the magnetic field. Further, in this figure the results of inelastic light-scattering experiments on a QWW of Goñi *et al.*<sup>13</sup> are plotted. It is remarkable that for the used sample the case of one occupied subband is realized for magnetic fields larger than 1.5 T. If one compares the theoretical RPA dispersion curve of the (1-0) intersubband magnetoplasmon with that obtained from resonant light scattering it is obvious that the RPA well describes the magnetic-field dependence of the measured curve. It is seen that the theoretical curve fits the lower field exper-

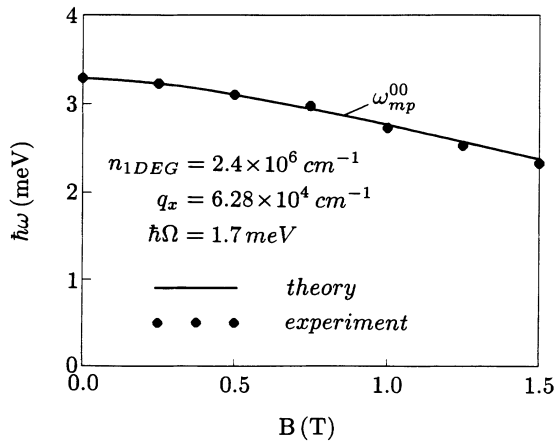


FIG. 2. Dispersion relation of the intrasubband magnetoplasmon branch  $\omega_{mp}^{00}$  as a function of the magnetic field. The calculated full RPA dispersion relation is given by the solid line. The symbols indicate the experimentally observed FIR transmission positions of Ref. 11. For the comparison of the theoretical and experimental dispersion curves, we fit  $\omega_p^{00}$  ( $B=0$ ) on the experimental value.

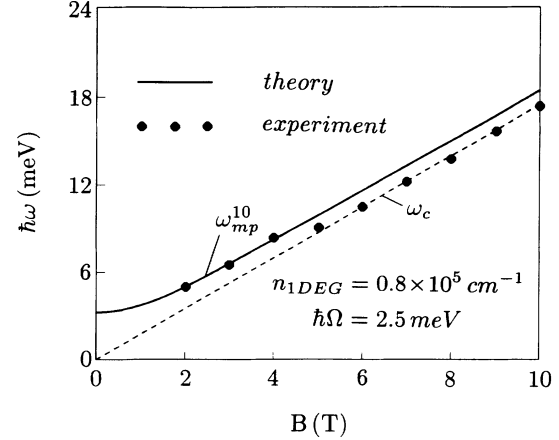


FIG. 3. Dispersion relation of the intersubband magnetoplasmon branch  $\omega_{mp}^{10}$  as a function of the magnetic field at  $q_x=0$ . The calculated full RPA dispersion relation is given by the solid line. The symbols represent the measured peak positions of resonant inelastic light-scattering spectra of Ref. 13. For the comparison of the theoretical and experimental dispersion curves we fit  $\omega_p^{10}$  ( $B=2$  T) on the experimental value.

imental results nearly perfect, but the theoretical curve does not approach the cyclotron frequency  $\omega_c$ , i.e., the 2D limit, so abruptly as the experimental results do. There are several reasons possible for this behavior in the experiment. Our model is based on a single QWW with an ideal parabolic potential of infinite height. In the experiment a lateral multiwire structure is used with a confining potential of finite height. Two additional effects arise: (i) the Coulomb coupling between the different wires and (ii) the finite width  $W$  of the confining potential restricts the center coordinate to  $Y_{k_x} \leq W/2$ . These two effects could be reasonable for the deviation of the theoretical curve from the experimental results at intermediate magnetic fields. The simple formula<sup>10</sup>  $\omega_{mp}^{10}(q_x=0) = \{[\omega_p^{10}(q_x=0)]^2 + \omega_c^2\}^{1/2}$  used by Goñi *et al.* for the magnetic-field dependence of the intersubband magnetoplasmon branch is of pure empirical nature for an effective ideal parabolic potential exact only for  $B=0$  and  $B=\infty$ . For a bare ideal parabolic potential this formula is an exact result for dipole-allowed transitions in far-infrared (FIR) transmission experiments but with  $\omega_p^{10}(q_x=0)$  equal to the bare subband difference.

Yang and Aers<sup>7</sup> used the time-dependent Hartree-Fock approximation to calculate the magnetoroton minimum which also was found in Ref. 13. It is found that the dispersion curve of the (1-0) intersubband magnetoplasmon is below the single-particle intersubband continuum, in differing from the experimental observation and our results. This could only be possible if the so-called excitonic shift of vertex corrections is larger in magnitude than the depolarization shift. But this is not to be expected for the density used.

Our theory is also in a good qualitative agreement with the recent observations of Drexler *et al.*<sup>12</sup> In this experiment the intersubband resonances ( $q_x=0$ ) are detected by FIR transmission spectroscopy. Because in the sample used between five and ten subbands, depending on the

magnetic field, are occupied, the three-subband model used here cannot be applied for a quantitative comparison. In this experiment a splitting of the mode  $\omega_{\text{mp}}^{10}$  in three modes above and below the frequency  $\omega = \sqrt{2}\omega_c$  is observed. In our opinion this behavior is caused by the nonparabolicity of the confining potential at higher gate bias.

In the long-wavelength limit it is possible to derive analytical expressions of the dispersion relation. To do this we use a two-subband model, i.e.,  $N, N' = 0, 1$ . If  $\xi k_F^{(0)} \ll 1$  ( $\xi = \gamma \tilde{l}_0 / \sqrt{2}$ ) it is possible to restrict the representation of the displaced center wave functions on two terms,  $L = 0, 1$  only. Using the long-wavelengths expressions of the matrix polarization function derived in Ref. 15, valid for realistic electron densities and in a broad range of the wave vector  $q_x / 2(k_F^{(0)} - \tilde{m}\omega / \hbar q_x) \ll 1$ , and the long-wavelength expressions for the matrix elements of the Coulomb potential ( $|q_x \tilde{l}_0| \ll 1$ ) in the dispersion relation, Eq. (2), we obtain two explicit dispersion relations. One describes the (0-0) intrasubband magnetoplasmon

$$\omega_{\text{mp}}^{00} = q_x \tilde{l}_0 \left[ \left( \frac{v_F^{(0)}}{\tilde{l}_0} \right)^2 - \frac{n_{\text{1DEG}} e^2}{2\pi \epsilon_0 \epsilon_s \tilde{m} \tilde{l}_0^2} \ln(|q_x \tilde{l}_0|) \right]^{1/2} \times \left\{ 1 + \frac{n_{\text{1DEG}} e^2 \omega_c^2}{2\Omega^2 (2\pi \epsilon_0 \epsilon_s \hbar \tilde{\omega}_c + n_{\text{1DEG}} e^2)} \right\}, \quad (6)$$

where the Fermi velocity is  $v_F^{(0)} = \hbar k_F^{(0)} / \tilde{m}$  and  $k_F^{(0)} = [2\tilde{m}(E_F - \mathcal{E}_0) / \hbar^2]^{1/2}$  is the Fermi wave vector. For vanishing magnetic field the expression (6) gives the known results for the intrasubband plasmon  $\omega_p^{00} = \omega_0(B=0)$ . The second dispersion relation is that of the (1-0) intersubband magnetoplasmon

$$\omega_{\text{mp}}^{10} = (1 + \alpha_{10})^{1/2} \tilde{\omega}_c, \quad (7)$$

with

$$\alpha_{10} = \frac{n_{\text{1DEG}} e^2}{2\pi \epsilon_0 \epsilon_s \hbar \tilde{\omega}_c} \left[ 1 - \frac{(\pi n_{\text{1DEG}} \gamma \tilde{l}_0)^2}{4} \right]. \quad (8)$$

The extra term in Eq. (8) is due to the depolarization effect. The depolarization shift increases with increasing magnetic field if the frequency  $\Omega$  of the confinement potential is larger than the critical frequency  $\Omega_c = \pi^2 n_{\text{1DEG}}^2 \hbar / (2m)$ . But if  $\Omega < \Omega_c$  is fulfilled,  $\alpha_{10} \tilde{\omega}_c^2$  has a minimum at  $\omega_c = (\Omega_c^{2/3} \Omega^{4/3} - \Omega^2)^{1/2}$ . For a GaAs QWW with  $n_{\text{1DEG}} = 1.9 \times 10^5 \text{ cm}^{-1}$  we have  $\hbar \Omega_c = 2 \text{ meV}$  and, hence, from the resulting minimum it should be possible to determine  $\Omega$  experimentally.

In summary, using the RPA for a Q1D Fermi liquid we have developed a perturbation scheme, free of any additional small parameter. This theory is able to describe well recent far-infrared transmission and inelastic light-scattering experiments with a good quantitative agreement. We have improved the theory of Li and Das Sarma<sup>6</sup> with which we are in qualitative agreement but our theory is valid in the whole experimental range of the parameters. The fairly good agreement of the RPA results with the experiment is evidence that the Q1DEG in the experimentally realized QWW's is adequately described as a Fermi liquid. Because the RPA results obtained here for the dispersion relations of the modes are always slightly above the measured curves, exchange and correlation could be responsible for this difference. In a forthcoming paper, we will use the scheme developed here for a theory of a collective excitation beyond the RPA to include exchange and correlation effects.

We gratefully acknowledge financial support by the Deutsche Forschungsgemeinschaft (DFG), Project No. We 1532/3-1.

<sup>1</sup>W. Que and G. Kirczenow, Phys. Rev. B **37**, 7153 (1989).

<sup>2</sup>Q. P. Li and S. Das Sarma, Phys. Rev. B **43**, 11 768 (1991).

<sup>3</sup>L. Wendler, R. Haupt, and R. Pechstedt, Phys. Rev. B **43**, 14 669 (1991).

<sup>4</sup>R. Haupt, L. Wendler, and R. Pechstedt, Phys. Rev. B **44**, 13 635 (1991).

<sup>5</sup>M. Bonitz, R. Binder, and S. W. Koch, Phys. Rev. Lett. **70**, 3788 (1993).

<sup>6</sup>Q. P. Li and S. Das Sarma, Phys. Rev. B **44**, 6277 (1991).

<sup>7</sup>S.-R. E. Yang and G. C. Aers, Phys. Rev. B **46**, 12 456 (1992).

<sup>8</sup>L. Wendler, T. Kraft, and V. G. Grigoryan (unpublished).

<sup>9</sup>G. Gumbs, D. Huang, and D. Heitmann, Phys. Rev. B **44**, 8084 (1991).

<sup>10</sup>T. Demel, D. Heitmann, P. Grambow, and K. Ploog, Phys. Rev. B **38**, 12 732 (1988).

<sup>11</sup>T. Demel, D. Heitmann, P. Grambow, and K. Ploog, Phys. Rev. Lett. **66**, 2657 (1991).

<sup>12</sup>H. Drexler, W. Hansen, J. P. Kotthaus, M. Holland, and S. P. Beaumont, Phys. Rev. B **46**, 12 849 (1992).

<sup>13</sup>A. R. Goñi, A. Pinczuk, J. S. Weiner, B. S. Dennis, L. N. Pfeiffer, and K. W. West, Phys. Rev. Lett. **70**, 1151 (1993).

<sup>14</sup>Q. Li, S. Das Sarma, and R. Joynt, Phys. Rev. B **45**, 13 713 (1992).

<sup>15</sup>L. Wendler and V. G. Grigoryan, Phys. Status Solidi B **181**, 133 (1994).